Link to published version (if available):
10.1038/nature06053

Link to publication record in Explore Bristol Research
PDF-document

No extreme bipolar glaciation during the main Eocene calcite compensation shift

Kirsty M. Edgar[1], Paul A. Wilson[1], Philip F. Sexton*[1] & Yusuke Suganuma[2]

[1]*National Oceanography Centre, School of Ocean and Earth Science, European Way, Southampton, SO14 3ZH, UK*

[2]*Department of Earth & Planetary Science, University of Tokyo, 7-3-1 Hongo Bunkyo-ku, Tokyo, 113-0033 Japan*

*Present address: Scripps Institution of Oceanography, University of California, San Diego, La Jolla, CA 92093-0244, USA and School of Earth, Ocean and Planetary Sciences, Cardiff University, Main Building, Park Place, Cardiff, CF10 3YE, UK.

Major ice sheets were permanently established on Antarctica approximately 34 million years ago[1-3], close to the Eocene/Oligocene boundary, at the same time as a permanent deepening of the calcite compensation depth in the world's oceans[4]. Until recently, it was thought that Northern Hemisphere glaciation began much later, between 11 and 5 million years ago[1-3,5]. This view has been challenged, however, by records of ice rafting at high northern latitudes during the Eocene epoch[6,7] and by estimates of global ice volume that exceed the storage capacity of Antarctica[8] at the same time as a temporary deepening of the calcite compensation depth ~41.6 million years ago[9]. Here we test the hypothesis

that large ice sheets were present in both hemispheres ~41.6 million years ago using marine sediment records of carbon and oxygen isotope values and of calcium carbonate content from the equatorial Atlantic Ocean. These records allow, at most, an ice budget that can easily be accommodated on Antarctica, indicating that large ice sheets were not present in the Northern Hemisphere. The records also reveal a brief interval shortly before the temporary deepening of the calcite compensation depth during which the calcite compensation depth shoaled, ocean temperatures increased, and carbon isotope values in the equatorial Atlantic decreased. The nature of these changes around 41.6 million years ago implies common links, in terms of carbon cycling, with events at the Eocene/Oligocene boundary[4] and with the 'hyperthermals' of the Early Eocene climate optimum[3,10,11]. Our findings help to resolve the apparent discrepancy between the geological records of Northern Hemisphere glaciation[6-8] and model results[12,13] that indicate that the threshold for continental glaciation was crossed earlier in the Southern hemisphere than in the Northern Hemisphere.

A striking feature of the composite[3] Cenozoic $\delta^{18}O$ record in benthic foraminiferal calcite is the abrupt increase in values across the Eocene/Oligocene boundary, 34 Myr ago (Fig. 1a). Together with evidence from Southern Ocean records for the initiation of ice rafting[14] and glacial weathering, and from sequence stratigraphic studies[15] for a global sea level fall (~70 m apparent sea level), this $\delta^{18}O$ shift is widely interpreted to signify the onset of major Antarctic glaciation[1-3,14] (Fig. 1a). The standard

view[1-3,5] is that substantial Northern Hemisphere glaciation occurred much later (Fig. 1a); recently, however, three lines of evidence have challenged this orthodoxy.

First, evidence for ice rafting in the Arctic Ocean around 45 Myr ago[6] and in the Norwegian-Greenland Sea between 37 and 27 Myr ago[7] (Fig. 1a). Second, new records for the Eocene/Oligocene boundary from the equatorial Pacific Ocean (ODP Leg 199 of the Ocean Drilling Program) show[4] that the amplitude of the $\delta^{18}O$ change ($\Delta\delta^{18}O_{benthic}$ = 1.5 ‰ VPDB) is impossibly large to be attributed to Antarctic glaciation alone. The simplest explanation for this result is that some of the $\Delta\delta^{18}O_{benthic}$ signal must denote global cooling[4]. However, Mg/Ca records[2,16] provide little support for declining temperatures. This raises the possibility of ice growth beyond Antarctica and/or the operation of some factor (such as changes in seawater carbonate chemistry associated with increasing calcite compensation depth, CCD) acting to mask the cooling signal in the Mg/Ca records[4,16]. Third, the $\delta^{18}O$ increase associated with the Eocene/Oligocene boundary occurred in lock-step with permanent deepening of the CCD, possibly in response to glacioeustatic sea level fall and reduced shelf carbonate accumulation[4]. Thus, the discovery[9,17] of multiple intervals of temporary CCD deepening in the equatorial Pacific earlier in the Eocene (Fig. 1b) has prompted speculation of transient glaciations before the Eocene/Oligocene boundary. A recent study[8] invokes three such glaciations including one extreme bipolar event (100 to 190 m apparent sea level change; ~35-70 $\times 10^6$ km^3 ice) coincident with the most prominent of the transient Eocene CCD deepening events (carbonate accumulation event CAE-3 ~41.6 Myr ago; ref 9 and Fig. 1b, c). Yet the idea that large ice sheets existed in both hemispheres at this time is at odds with contemporaneous warm polar ocean temperatures[3,18], high

atmospheric CO_2 levels[19] (Fig. 1a) and the occurrence of (sub)tropical flora at mid- to

high latitudes[20]. Sequence stratigraphic records[21] support the concept of early Cenozoic

glaciations, but the ice sheets invoked are much more modest in size (~10 to 45 m

apparent sea level change; ~ 40 to 65 % of present East Antarctic ice sheet) and

considered compatible with high-latitude warmth because of their restriction to the

interior of Antarctica[21].

Although the sensitivity to CCD change[17] of the Pacific drill sites used to infer

extreme bipolar Eocene glaciation is beneficial to understanding carbon cycling, it is

detrimental to generating isotope records from calcareous microfossils whose

occurrence and preservation are sensitive to changes in carbonate saturation state. Thus,

further tests of bipolar Eocene glaciation are warranted. We generated high-resolution

(~ 4.5 kyr) monospecific stable isotope records for the interval spanning CAE-3 (ref 9)

from the equatorial Atlantic Ocean (ODP Leg 207, Demerara Rise, Site 1260, 9°16'N,

54°33'W; palaeowater depth 2500-3000 m)[22]. These sediments were deposited well

above the local CCD for most of the study interval and are shallowly buried[22] favouring

calcareous microfossil preservation[18].

In Figure 1c-e, we compare our new $\delta^{18}O$ records from the equatorial Atlantic

with the record presented[8] from the equatorial Pacific in support of bipolar glaciation.

$\delta^{18}O$ data from the equatorial Pacific show a considerable spread, and the amplitude of

increase used to infer extreme bipolar glaciation relies on outliers in sparse data

($\Delta\delta^{18}O_{benthic}$ = 1.2 ‰ VPDB, arrows, Fig. 1c). Our data from the Atlantic are more

continuous and show less spread (Fig. 1d, e). Our benthic record (Fig. 1d) shows a well-

defined minimum around the middle of magnetochron C19r followed by a shift to higher values attained by the onset of CAE-3 (zone I/II boundary, Fig. 1c). Our planktic record shows a similar pattern (Fig. 1e). One interpretation of the correspondence between our planktic and benthic records is that it reflects an increase in the oxygen isotope composition of seawater ($\delta^{18}O_{seawater}$) and supports the notion of ice growth. Another interpretation, arguably more in keeping with the other palaeoclimate records[19] and numerical modelling results[12,13] shown in Figure 1a, is that our data are attributable to cooling of surface and bottom waters at Site 1260. Regardless, our estimate of the $\Delta\delta^{18}O_{benthic}$ signal associated with CAE-3 is about half that proposed[8] from the Pacific (Fig. 1d versus 1c).

In Figure 2 we show the relationship between measured $\Delta\delta^{18}O_{benthic}$ and global continental ice volumes for a range of values for mean $\delta^{18}O$ of stored ice ($\delta^{18}O_{ice}$). Horizontal dashed lines denote different values for $\Delta\delta^{18}O_{benthic}$, vertical solid lines correspond to different values assumed for $\delta^{18}O_{ice}$ and intersections yield the resulting estimated ice volumes (see 'isovols' lines). Lines a and b assume that the whole $\Delta\delta^{18}O_{benthic}$ signal is attributable to ice volume. Assuming, that $\delta^{18}O_{ice}$ was as extreme as today (about −50 ‰ SMOW[4,23]) the $\Delta\delta^{18}O_{benthic}$ signal inferred in the Pacific study[8] for CAE-3 (line a in Fig. 2) yields a global middle Eocene ice budget almost 1.5 times the present Antarctic ice volume (25.4 ×10^{6} km[3])[24]. However, the latitudinal temperature gradient during the Eocene was less extreme than today so it is likely that $\delta^{18}O_{ice}$ was also less extreme (conservatively about −30‰ SMOW[4,23,25]), yielding even larger ice budgets (almost 2.5 times the modern Antarctic budget). This ice volume is close to the global total estimated for the last glacial maximum (Fig. 2) when large ice sheets existed

not only on Antarctica and Greenland but also over large areas of North America and Eurasia, and it implies an even greater global ice budget for the Eocene/Oligocene boundary when benthic $\delta^{18}O$ values were ~0.8 ‰ higher (Fig. 1a). Even larger ice volumes were invoked[8] for CAE-3 in the Pacific study using the dual benthic Mg/Ca – $\delta^{18}O$ method ($\Delta\delta^{18}O_{seawater}$ = 1.5 ‰). But we focus on the $\Delta\delta^{18}O_{benthic}$ signal alone because the presence of authigenic dolomite[16,17] towards the base of the section at ODP Site 1218 means that the only potentially meaningful Mg/Ca data published for CAE-3 are for its termination (see Fig. 3 of ref. 8). By focusing on the $\Delta\delta^{18}O_{benthic}$ signal alone we adopt a conservative approach because the ice budgets calculated in this way in ref. 8, although extreme (because the whole signal was attributed to ice growth with no associated cooling), are less extreme than those that were estimated by the dual benthic Mg/Ca – $\delta^{18}O$ method.

If we assume no cooling component associated with the smaller $\Delta\delta^{18}O_{benthic}$ signal seen in our new record (line b, Fig. 2), our revised estimate of the upper limit of possible ice growth associated with CAE-3 is correspondingly smaller, and it need not require ice storage in the Northern Hemisphere and it is more in keeping with sequence stratigraphy records[21]. On this basis, we cannot exclude the possible existence of small valley glaciers draining the uplands of Greenland around 41.6 Myr ago, particularly in light of dropstones recently discovered[6,7] in Eocene strata in the high northern latitudes. Nevertheless, we can rule out the existence of large ice sheets in the Northern Hemisphere and we therefore find no support for extreme Eocene bipolar glaciation. Based on work elsewhere[23,26] we might expect the $\Delta\delta^{18}O_{benthic}$ signal to be composed of at least equal parts ice volume and temperature (line b', Fig. 2). On this basis we

calculate ice budgets that are easily accommodated on central Antarctica alone (~0.4 to 0.6 times modern Antarctic budget). Under these circumstances, only by assuming an extremely high value for $\delta^{18}O_{ice}$ akin to the average for high altitude glaciers in the temperate zone today (≥ -15‰ SMOW) does the calculated ice volume exceed the modern budget for Antarctica (Fig. 2).

The main reason why the ice budgets of ref. 8 are so large is because their estimate of $\Delta\delta^{18}O_{benthic}$ was based on outlying data points and their isotope record is particularly sparse towards the top of magnetochron C19r (note the coring gap on the run up to CAE-3 and inferred glaciation, zone I/II boundary in Fig. 1c). To assess this interval in more detail we show an expanded version of our foraminiferal $\delta^{18}O$ series together with accompanying $\delta^{13}C$, lithological and bulk sediment records in Fig. 3. Excursions to lower values of $\delta^{18}O$ (by ~ 0.4 ‰) and $\delta^{13}C$ (by 1.2 to 1.5 ‰) occur in both benthic and planktic records. These are accompanied by prominent decreases in bulk $\delta^{18}O$ (by 1.8 ‰) and $\delta^{13}C$ (by 1.1 ‰) within magnetochron C19r, across a 30 cm interval containing a highly dissolved foraminiferal assemblage and a well-developed red clay horizon where carbonate content falls sharply from ~75 weight percent $CaCO_3$ to a minimum of about 35 weight percent $CaCO_3$ (Fig. 3f). This event goes undetected in the equatorial Pacific record presumably because it falls in the core gap at ODP Site 1218 (Fig. 1c) and therefore cannot explain the discrepancy between the two $\Delta\delta^{18}O_{benthic}$ signals shown in Figure 1. On the other hand, our records show that, while ODP Site 1260 remained above the CCD for the vast majority of the study interval, shortly before the CCD deepened in the equatorial Pacific (CAE-3 in Fig. 1), it shoaled in the equatorial Atlantic sufficiently to be readily detectable at a water depth of about 3.0 to

2.5 km. In this respect, our records resemble those for the Eocene/Oligocene boundary where the CCD shoals sufficiently to completely eliminate $CaCO_3$ burial at ODP Site 1218 for ~200 kyrs immediately before the rapid two-step deepening associated with Antarctic glaciation (see figure 1 of ref. 4).

We cannot yet determine whether the C19r event is global in occurrence because of the coring gap at ODP Site 1218 and radiolarian clays and low sedimentation rates ($\leq$ 0.2 cm/kyr) at other key drill sites in the Equatorial Pacific[17] and on Shatsky Rise[27]. But it is distinct from the much longer-lived Middle Eocene Climate Optimum already documented at Site 1260[18] and it is more similar in expression to the well-known intervals of rapid carbon-cycle-led global warming and CCD shoaling in the early Paleogene. The magnitude of the palaeoceanographic signals that we have documented for magnetochron C19r at Site 1260 is smaller than seen at the Paleocene/Eocene boundary[3,10] but at least as large as those marking the Eocene Thermal Maximum 2 (~53 Myr ago)[11].

Our findings appear to highlight the instability of Eocene climate and to emphasize close coupling to the carbon cycle as expressed in oceanic carbonate saturation and $\delta^{13}C$. If the interval of CCD shoaling and isotopic shifts that we document is substantiated elsewhere, our results suggest that carbon cycle-led instabilities akin to those documented in the early Eocene were not restricted to the Cenozoic climate optimum but also occurred millions of years later when the Earth's baseline climate had cooled substantially and was poised much closer to the threshold of continental glaciation (Fig. 1a). Climate modelling experiments suggest[12,13] that this

threshold would have been crossed earlier in the Southern Hemisphere than in the Northern Hemisphere (Fig. 1a) because of the fundamentally different land-ocean distributions at the two poles. Our work helps to re-align the geologic record with this view.

Methods

Chronology. We use the published[28] palaeomagnetic reversal stratigraphy for ODP Site 1260, which we supplemented by analysing nearly 100 additional samples collected at approximately 20 to 30 cm intervals across each of the magnetic reversals in the studied stratigraphic interval (magnetochrons C20r through C18r). Methods are as in ref. 28.

CaCO$_3$ and stable isotope data. All data were generated at the National Oceanography Centre, Southampton, UK . Bulk sediment weight %CaCO$_3$ was measured on small (20-30 mg) discrete samples (1-5 cm spacing), by high-precision coulometry. Our foraminiferal stable isotope (δ^{18}O and δ^{13}C) data were generated using species separates of the benthic and planktic foraminifera *Cibicidoides eoceanus* and *Morozovella lehneri* respectively. Foraminifera were cleaned by ultrasonication prior to analysis. Benthics were picked from the size range 300-450 μm while planktics were picked from the 250-300 μm size fraction. Bulk stable isotope measurements were generated on splits of the same samples used for CaCO$_3$ data. All stable isotope measurements were determined using a Europa GEO 20-20 mass spectrometer equipped with an automatic carbonate preparation system (CAPS). Results are reported relative to the Vienna Pee Dee Belemnite (VPDB) standard with an external analytical precision, based on replicate analysis of an in-house standard calibrated to NBS-19, better than 0.1‰ for δ^{18}O and δ^{13}C. Benthic δ^{18}O values that we report from ODP Site 1260 have been adjusted to

equilibrium by adding 0.28‰ VPDB, the Palaeogene correction factor for *Cibicidoides*. We plot *Cibicidoides* data from ODP Site 1218 in the same way to aid comparison (Site 1218 data from *Nuttallides truempyi* are reported in the same way as in ref. 8).

1.   Miller, K. G., Wright, J. D. & Fairbanks, R. G. Unlocking the Ice House: Oligocene-Miocene Oxygen Isotopes, Eustasy, and Margin Erosion. *J. Geophys. Res.* **96**, 6829-6848 (1991).

2.   Lear, C. H., Elderfield, H. & Wilson P, A. Cenozoic Deep-Sea Temperatures and Global Ice Volumes from Mg/Ca in Benthic Foraminiferal Calcite. *Science* **287,** 269-272 (2000).

3.   Zachos, J., Pagani, M., Sloan, L., Thomas, E. & Billups, K. Trends, Rhythms, and Aberrations in Global Climate 65 Ma to Present. *Science* **292**, 686-693 (2001).

4.   Coxall, H. K., Wilson, P. A., Pälike, H., Lear, C. H. & Backman, J. Rapid stepwise onset of Antarctic glaciation and deeper calcite compensation in the Pacific Ocean. *Nature* **433**, 53-57 (2005).

5.   Holbourn, A., Kuhnt, W., Schulz, M. & Erlenkeuser, H. Impacts of orbital forcing and atmospheric carbon dioxide on Miocene ice-sheet expansion. *Nature* **438**, 483-487 (2005).

6.   Moran, K. *et al*. The Cenozoic palaeoenvironment of the Arctic Ocean. *Nature* **441**, 601-605 (2006).

7.   Eldrett, J. S., Harding, I. C., Wilson, P. A., Butler, E. & Roberts, A. P. Continental ice in Greenland during the Eocene and Oligocene. *Nature* **446,** 176-179 (2007).

8.   Tripati, A., Backman, J., Elderfield, H. & Ferretti, P. Eocene bipolar glaciation associated with global carbon cycle changes. *Nature* **436**, 341-346 (2005).

9.   Lyle, M., Olivarez Lyle, A., Backman, J. & Tripati, A. Biogenic Sedimentation in the Eocene Equatorial Pacific - The Stuttering Greenhouse and Eocene Carbonate Compensation Depth. *Proc. ODP Sci. Res.* (eds. Wilson, P. A., Lyle, M. & Firth, J. V.) **199**, 1-35 (Online) (2005).

10.   Zachos, J. C. *et al.* Rapid Acidification of the Ocean During the Paleocene-Eocene Thermal Maximum. *Science* **308**, 1611-1615 (2005).

11.   Lourens, L. J. *et al*. Astronomical pacing of late Palaeocene to early Eocene global warming events. *Nature* **435**, 1083-1087 (2005).

12.   DeConto, R. M. & Pollard, D. Northern Hemisphere Glaciation in the early Cenozoic? *AGU Fall Meeting 2006*, abstract #PP21B-1678 (2006).

13.   DeConto, R. M. & Pollard, D. Rapid Cenozoic glaciation of Antarctica induced by declining atmospheric CO_2. *Nature* **421,** 245-249 (2003).

14.   Zachos, J. C., Breza, J. R. & Wise, S. W. Early Oligocene ice-sheet expansion on Antarctica: Stable isotope and sedimentological evidence from Kerguelen Plateau, southern Indian Ocean. *Geology* **20**, 569-573 (1992).

15.   Pekar, S. F., Christie-Blick, N., Kominz, M. A. & Miller, K. G. Calibration between eustatic estimates from backstripping and oxygen isotopic records for the Oligocene. *Geology* **30**, 903-906 (2002).

16.   Lear, C. H., Rosenthal, Y., Coxall, H. K. & Wilson, P. A. Late Eocene to early Miocene ice sheet dynamics and the global carbon cycle. *Paleoceanography* **19**, doi: 10/1029/2004PA001039 (2004).

17.   Shipboard Scientific Party 2002. Leg 199 Summary. *Proc. ODP Init. Rep.* (eds. Lyle, M., Wilson, P. A., Janecek, T. R.) **199**, 1-87 (2002).

18.   Sexton, P. F., Wilson, P. A., & Norris, R. D. Testing the Cenozoic multi-site composite $\delta^{18}O$ and $\delta^{13}C$ curves: new Eocene monospecific records from a single locality, Demerara Rise (ODP Leg 207). *Paleoceanography* **21**, PA2019, doi:10.1029/2005PA001253 (2006).

19.   Pagani, M., Zachos, J. C., Freeman, K. H., Tipple, B. & Bohaty, S. Marked Decline in Atmospheric Carbon Dioxide Concentration During the Paleogene *Science* **309**, 600-603 (2005).

20.   Wolfe, J. A. in *The carbon cycle and atmospheric CO_2; Natural variations Archean to Present.* (eds Sundquist, E. T. & Broecker, W. S.) 357-375 (Geophys. Mono. 32, American Geophysical Union, Washington DC, 1985).

21.   Pekar, S. F., Hucks, A., Fuller, M. & Li, S. Glacioeustatic changes in the Early and Middle Eocene (51-42 Ma): Shallow-water stratigraphy from ODP Leg 189 Site 1171 (South Tasman Rise) and deep-sea $\delta^{18}O$ records. *Geol. Soc. Am. Bull.* **117**, 1081-1093 (2005).

22.   Shipboard Scientific Party 2004. Leg 207 Summary. *Proc. ODP Init. Rep.* (eds. Erbacher, J., Mosher, D. C., Malone, M. J.) **207**, 1-89 (2004).

23.   Pekar, S. F., DeConto, R. M. & Harwood, D. M. Resolving a late Oligocene conundrum: Deep-sea warming and Antarctic glaciation. *Palaeogeogr. Palaeoclimatol. Palaeoecol.* **231**, 29-40 (2006).

24.   Lythe, M. B., Vaughan, D. G. & consortium, B. BEDMAP: A new ice thickness and subglacial topographic model of Antarctica. *J. Geophys. Res.* **106**, 335-351 (2001).

25.   Poulsen, C. J., Pollard, D. and White, T. S. General circulation model simulation of the $\delta^{18}O$ content of continental precipitation in the middle Cretaceous: A model-proxy comparison. *Geology* **35**, 199-202 (2007).

26.   Schrag, D. P. *et al*. The oxygen isotopic composition of seawater during the Last Glacial Maximum. *Quat. Sci. Rev.* **21**, 331-342 (2002).

27.   Shipboard Scientific Party. Leg 198 Summary. *Proc. ODP Init. Rep.* (eds. Bralower, T. J., Premoli-Silva, I., Malone, M. J.) **198**, 1-148 (2002).

28.   Suganuma, Y. & Ogg, J. G. Campanian through Eocene Magnetostratigraphy of Sites 1257-1261, ODP Leg 207, Demerara Rise (Western Equatorial Atlantic). *Proc. ODP Sci. Res.* (eds. Mosher, D. C., Erbacher, J. & Malone, M. J.) **207**, 1-48 (online) (2006).

29.   Pälike, H. *et al*. The Heartbeat of the Oligocene Climate System. *Science* **314**, 1894-1898 (2006).

30.   Huybrechts, P. Sea-level changes at the LGM from ice-dynamic reconstructions of the Greenland and Antarctic ice sheets during the glacial cycles. *Quat. Sci. Rev.* **21**, 203-231 (2002).

Figure 1 Palaeoceanographic records showing changes in ocean chemistry and global climate. **a,** Cenozoic atmospheric CO_2[19], grey shading defines the range of estimated CO_2 values as calculated in ref. 19 relative to the pre-anthropogenic level (PAL). Vertical dashed blue lines are model-defined thresholds for large ice sheet initiation. SHG and NHG, Southern and Northern Hemisphere glaciation[12,13]. Composite benthic $\delta^{18}O$ record[3]. Vertical blue bars show the standard view of the presence and extent of full-scale/permanent ice sheets (solid bars) and those thought to have been partial/ephemeral (broken bars). Occurrences of newly documented ice rafted debris (IRD) from the high northern latitudes are also shown[6,7]. EECO, Early Eocene Climatic Optimum. **b,** $CaCO_3$ mass accumulation rate (MAR) for the equatorial Pacific[9,29]. The inset shows the classic CCD record for the equatorial Pacific 50 Myr ago to the

present, with the pink-shaded zone indicating the interval of transient CCD events[9]. Epochs are indicated (abbreviated) to the left of **a** and in the inset. **c,** Benthic $\delta^{18}O$ record from ODP Site 1218 (the dark green data points are from ref. 8 and yellow ones are from ref. 16). The shaded grey zones are; I, pre-onset of CAE-3; II = onset-to-peak $CaCO_3$ mass accumulation rate during CAE-3; III = post-peak $CaCO_3$ mass accumulation rate during CAE-3. Red arrows denote data points defining[8] 1.2 ‰ amplitude of $\delta^{18}O$ increase ($\Delta\delta^{18}O$) and thus hypothesised extreme bipolar glaciation. **d**, **e**, New benthic and planktic $\delta^{18}O$ records from ODP Site 1260. Median values (white lines) and 1σ variance (shaded envelopes) are shown in **c**, **d** and **e**. Vertical dashed red lines in **d** denote our smaller estimate of $\Delta\delta^{18}O$ (~ 0.6 ‰ VPDB), derived from the maximum and minimum values in the 1σ envelope of the benthic record. Magnetochrons are indicated to the left of **c**.

Figure 2 Measured increases in $\delta^{18}O$ in benthic foraminifera ($\Delta\delta^{18}O$ $_{benthic}$) and resulting global continental ice volumes for a range of values for the mean $\delta^{18}O$ of stored ice ($\delta^{18}O_{ice}$). Horizontal dashed lines indicate different values for $\Delta\delta^{18}O_{benthic}$ described in the text and assume $\Delta\delta^{18}O_{benthic}$ = 100 % ice volume (a = equatorial Pacific[8]; b = equatorial Atlantic, this study). Thick vertical lines correspond to different values of $\delta^{18}O_{ice}$ (estimated $\delta^{18}O_{ice}$ today −50 ‰ and for the middle Eocene −30 ‰). Intersections yield resulting calculated ice volume shown by 'isovols' (values shown $\times 10^6$ km^3). The horizontal dashed line labelled b' corresponds to $\Delta\delta^{18}O_{benthic}$ = 0.6 ‰, with 50 % of that signal attributable to ice. Present Antarctic ice volume (PAIV)[24], Antarctic ice volume at

the LGM (ALGM)[30] and total global ice volume at the Last Glacial Maximum (GLGM) shown for reference. SMOW, standard mean ocean water.

Figure 3 Palaeoceanographic records from ODP Site 1260 showing the run up to CAE-3. We note the short-lived interval of CCD shoaling and ocean warming around 75 metres composite depth. **a,** Benthic δ^{13}C data. **b,** Planktic δ^{13}C data. **c,** Benthic δ^{18}O data. **d**, Planktic δ^{18}O data. **e,** Bulk sediment lightness (L*)[22]. **f,** Bulk sediment weight %CaCO$_3$. **g,** Bulk sediment δ^{13}C. **h,** Bulk sediment δ^{18}O. Question marks in **a-d** denote absence of two to three samples because of the lack of suitable foraminifera for analysis in this interval. Grey shaded zones I and II as in Fig. 1.
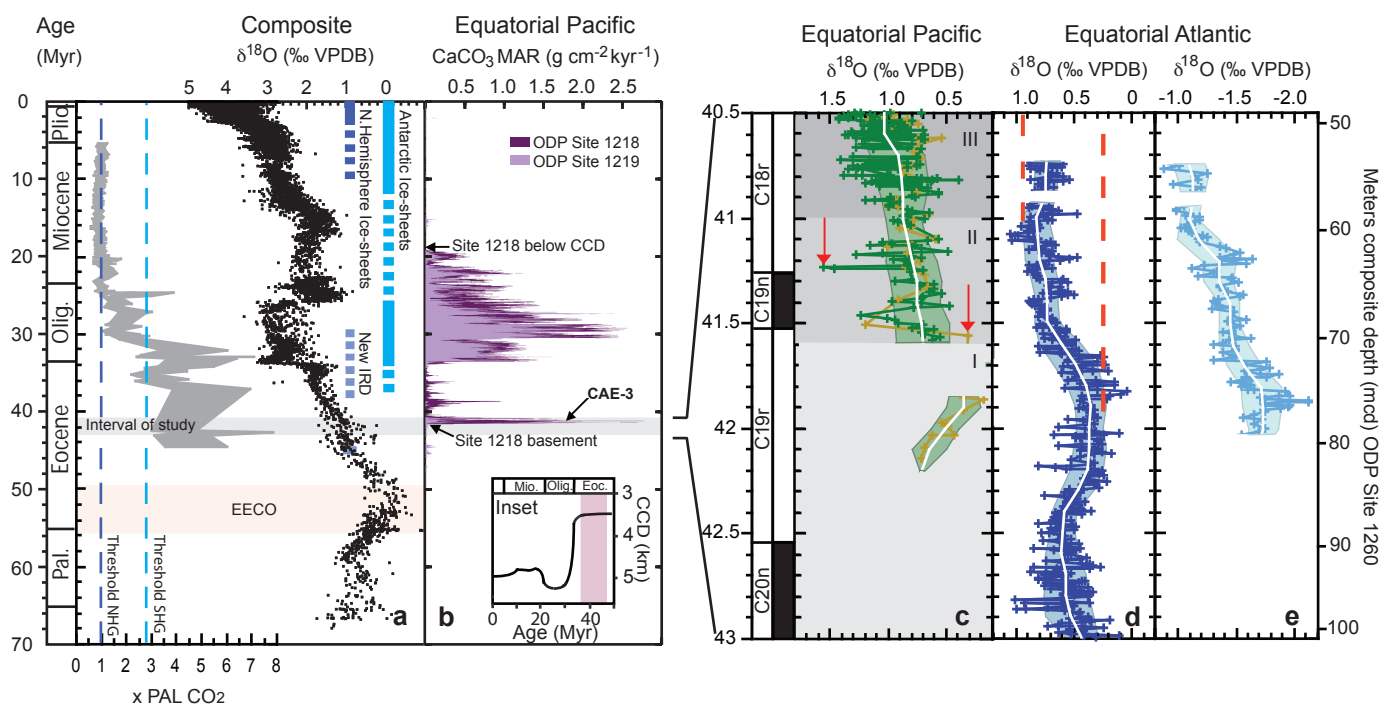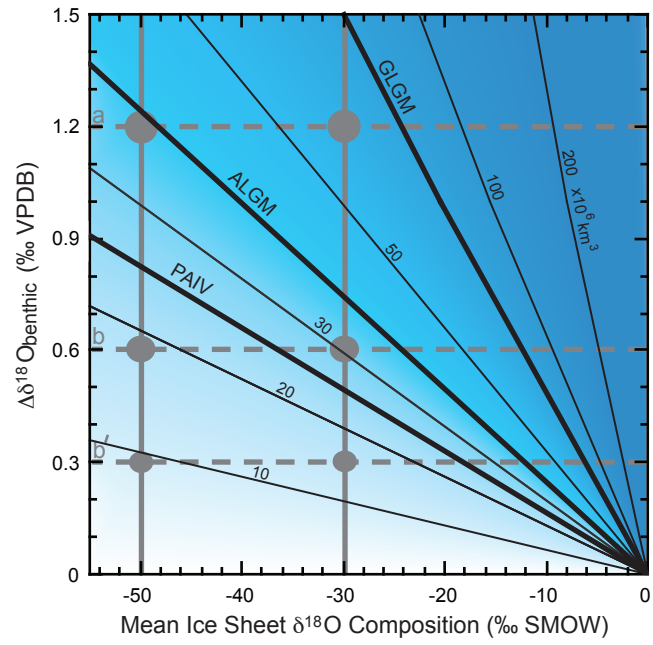
FIGURE 1

Age (Myr)

Composite δ¹⁸O (‰ VPDB)

Equatorial Pacific CaCO₃ MAR (g cm⁻² kyr⁻¹)

Equatorial Pacific δ¹⁸O (‰ VPDB)

Equatorial Atlantic δ¹⁸O (‰ VPDB)

FIGURE 2

FIGURE 3